Colloid Polym Sci (2002) 280:454–460
DOI 10.1007/s00396-001-0633-4

Tsuneo Okubo
Shinya Okuda
Hiroshi Kimura

Dissipative structures formed in the course of drying the colloidal crystals of silica spheres on a cover glass

Received: 8 August 2001
Accepted: 9 November 2001

Presented at the Annual Meeting of the Society of Fiber Science and Technology, Japan, Kyoto, June 7–9, 2000

T. Okubo (✉) · S. Okuda · H. Kimura
Department of Applied Chemistry and
Graduate School of Materials Science
Gifu University, Gifu 501–1193, Japan
E-mail: okubotsu@apchem.gifu-u.ac.jp

Abstract Macroscopic and microscopic dissipative structural patterns formed in the course of drying the deionized aqueous colloidal crystal suspensions of silica spheres (diameter: 103 nm) on a cover glass have been observed. Spoke-like and ring-like patterns are formed in the macroscopic scale; the former is the crack in the sphere film and the latter is the hill accumulated with spheres formed around the outside edge. The neighbored inter-spoke angle, thickness of the film, and other morphological parameters have been discussed as a function of sphere concentration, concentration of sodium chloride, and the inclined angle of the cover glass. Fractal patterns of the mud cracks are observed in the microscopic scale. Capillary forces between spheres at the air-liquid surface and the relative rates between the water flow at the drying front and the convection flow of spheres are important for the pattern formation.

Keywords Dissipative structure · Pattern formation · Drying colloidal crystal suspensions · Colloidal silica spheres · Fractal pattern

Introduction

It is well known that most patterns in nature and experiments in laboratory are formed via self-organization in the course of dissipation of free energy and in the non-equilibrium state. Among the so many factors for the free energy dissipation, evaporation and convection induced by the earth gravity are very important for the pattern formation.

Colloidal crystallization phenomena, which are not dissipative structures but typical examples of the three-dimensional self-organization in the thermodynamically equilibrium state, have been studied intensively by many researchers including the authors' group [1, 2, 3, 4, 5, 6, 7, 8, 9, 10]. It has been clarified that the structural and kinetic properties of the colloidal crystals are influenced strongly by the electrostatic inter-particle interaction via the electrical double layers around the particles, shape of colloidal particles, and the interaction between the particles and the cell wall of a sample container. For example, the most dense crystal planes, 111 and 100 crystal planes for the face-centered-cubic (fcc) and body-centered-cubic (bcc) lattices, always orient parallel to the cell wall. Furthermore, colloidal crystallization rates are much higher for the plane cell than those for the curved cuvette cell.

Several papers on the pattern formation in the course of drying of the monodispersed colloidal suspensions have been reported so far [11, 12, 13, 14, 15, 16, 17, 18, 19, 20, 21, 22, 23, 24, 25, 26]. Most of the papers have studied the liquid-like suspensions containing more or less ionic species. As the important factors of dissipation interactions, electrostatic inter-particle interactions have been identified. Hydrophobic and hydrophilic interactions are also demonstrated to be important for the drying process [16, 24, 25]. Gelbart et al. [14, 15, 17] examined the mechanism of solvent dewetting in annular ring structures formed by drying a diluted metal colloid on a substrate. Shimomura et al. and other researchers have studied intensively the dissipative patterns in the processes of film formation by drying of the polymer solutions [27].

In this work the dissipative patterns have been observed in the course of drying colloidal crystal suspensions of monodispersed silica spheres on a cover glass. The colloidal crystal suspensions are undoubtedly one of the most simple and convenient systems for study of the dissipative structures on a laboratory scale. For example, the structural information in the processes of the dissipative pattern formation from the colloidal crystals is available by reflection spectroscopy in detail as is shown in this work.

Experimental

Materials. Colloidal silica spheres, CS-82 were kindly donated from Catalyst & Chemicals Co. (Tokyo). The diameter, standard deviation (δ) from the mean diameter, and the polydispersity index (δ/d_o) were 103 nm, 13.2 nm, and 0.13, respectively. The colloidal sample was first purified several times using an ultrafiltration cell (Model 202, Diaflo-XM300 membrane, Amicon Co.), and then deionized by coexistence with a mixed bed of cation- and anion-exchange resins more than five years before use. They released an amount of alkali from their surfaces. It takes a long time before complete deionization is achieved, since the deionization proceeds between the two solid-liquid phases one after another, i.e., between colloidal spheres and water and then between water and the resins. The values of δ and d_o were determined through the courtesy of Nippon Synthetic Rubber Co. (Tokyo) by electron microscopy. The surface density of strongly acidic charges of these spheres was determined to be 0.38 μC/cm^2 by the conductometric titration with a Horiba Model DS-14 conductivity meter (Kyoto).

The water used for the sample preparation was purified by a Milli-Q reagent grade system (Milli-RO5 plus and Milli-Q plus, Millipore, Bedford, Mass.).

Observation of the dissipative structures. A volume of 0.2 ml of the aqueous suspension of CS-82 spheres was dropped carefully and gently on a micro cover glass (30 mm×30 mm, thickness No.1, 0.12–0.17 mm, Matsunami Glass Co., Kishiwada, Osaka) in a schale (60 mm in diameter, 15 mm in depth, Petri Co., Tokyo). The cover glass was used without further rinse. The contact angle for the pure water was $31 \pm 0.2°$ from the drop profile of water on the cover glass. The drop formed within a closed box made of thin glass coexisted with water in the bottom of the box. The experiments on the rinsed cover glasses having various contact angles are now in progress in our laboratory. The influence of the rinse on the dissipative patterns is significant from our preliminary experiments. A pipette (1-ml, disposable serological pipette, Corning Lab. Sci. Co.) was used for the dropping. Macroscopic and microscopic observation was made for the film formed after the suspension was dried up completely on a cover glass in a room air-conditioned at 25 °C and 65% humidity in air. To incline a cover glass, several sheets of the cover and slide glasses were inserted under one end of the schale. The degree of the inclination changed from 0° to 8°. Concentrations of the colloidal spheres and sodium chloride ranged from 1.33×10^{-9} to 0.05 in volume fraction and from 1×10^{-6} mol/l to 1×10^{-4} mol/l, respectively.

Macroscopic dissipative structures have been observed with a video camera recorder (CCD-V800, Sony) and a Canon EOS 10 camera with macro-lens (EF 50 mm, f = 2.5) and a life-size converter EF. Microscopic structures were observed with two digital HD microscopes (type VH-7000, Keyence Co., Osaka), a laser 3D profile microscope (type VK-8500, Keyence) and a Metallurgical microscope (Axiovert 25CA, Carl-Zeiss, Jena GmbH). Observation with an atomic force microscope (type SPA400, Seiko Instruments) was also made.

Reflection spectroscopy. Reflection spectra were taken perpendicularly to the colloidal films developed on a cover glass. A light beam from a halogen lamp (Hayashi LA-150SX, Tokyo) hits the sample using a Y-type optical fiber cable and the reflected light is measured on a multi-channel photo detector (type MCPD-7000G3, Otsuka Electronics, Hirakata, Osaka).

Results and discussion

Macroscopic patterns

Figure 1 shows the typical patterns formed in the drying the suspension of CS-82 spheres at the sphere concentrations ranging from 1.33×10^{-7} to 3.33×10^{-2} in volume fraction. At low sphere concentrations the islands of sphere regions, which distribute roundly, appeared. On the other hand, at high sphere concentrations at 0.0133 and 0.0333 in volume fraction the spoke-like cracks were

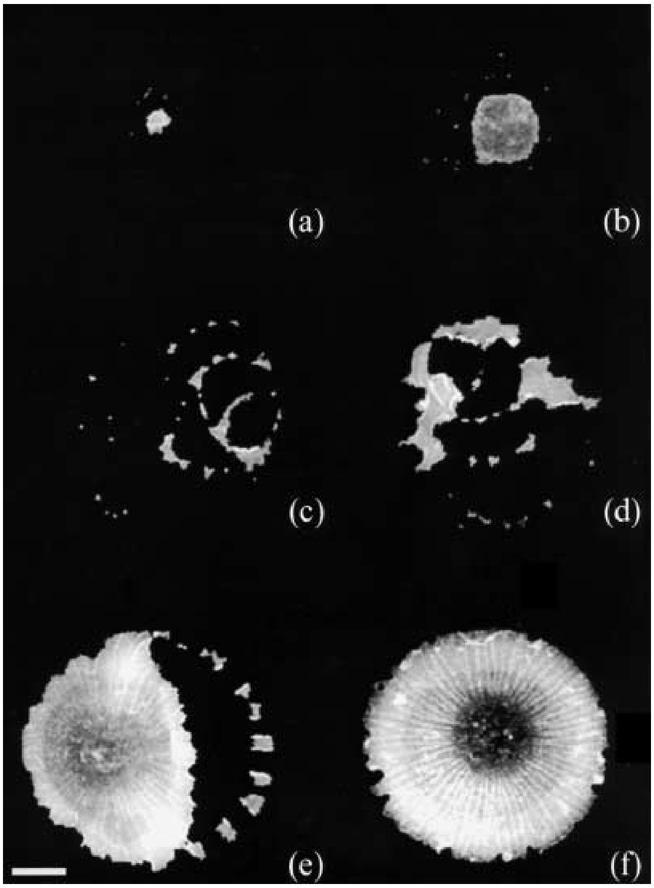

Fig. 1a–f Patterns formed for CS-82 spheres on a cover glass at 25 °C: **a** $\phi = 1.33\times10^{-7}$; **b** 1.33×10^{-5}; **c** 1.33×10^{-3}; **d** 6.67×10^{-3}; **e** 1.33×10^{-2}; **f** 3.33×10^{-2}. In water, 0.1 ml, length of the *bar* is 2.0 mm

formed from the outside edge toward the center. Clearly the cracks were formed in the process of shrinking of the wetted films [28, 29].

There were quite a few spheres in the central region in Fig. 1f, whereas broad ring-like region was occupied with the spheres. Narrow ring patterns were observed when the amount of the drop was low, 0.01 ml, for example, though the picture showing this was omitted in this paper. The authors observed that the spoke-like and the ring patterns were also observed for the deionized aqueous suspensions of monodispersed polystyrene spheres and India ink [30, 31].

A main cause for the ring formation is due to the convection flow of the solvent and the colloidal spheres. In particular, flow of the colloidal spheres from the center area toward the outside edges in the lower layer of the liquid drop, which is induced by the evaporation of water at the liquid surface, resulted in lowering of the suspension temperature in the upper region. When the spheres reach the edges of the drying frontier at the outside region of the liquid, part of the spheres will turn upward and go back to the center region. However, when most of the spheres reach the frontier region, the movement of the spheres may stop with the disappearance of water. This process must be followed by the ring-like accumulation of the spheres near the round edges. It should be noted here that the importance of the convection flow of colloidal spheres in the ring formation has often been observed in the process of film formation [19, 32].

The angles between the adjacent spoke-like cracks (θ) increased linearly as sphere concentration increased, though the graph showing this was omitted in this paper. Increase in sphere concentration will result in the increase in the elastic modulus of the film, and then in the increase in the θ-value. At 0.2 ml of $\phi = 0.0333$, for example, θ-values were $11.1° \pm 0.2°$, which means 32 ($= 360/11.1$) spoke-like cracks are formed in the pattern. The θ-values increased as the amount of the suspension drop increased, i.e., $\theta = 6.0°$, 6.8°, and 11.1° were observed for the drop amounts of 0.1 ml, 0.15 ml, and 0.2 ml. This observation will also be explained with the increased elastic modulus of the film, since the area of the film increased only slightly as the amount of the liquid drop increased. The area (S) values were 12, 41, 77, and 95 mm^2 when the liquid amounts at $\phi = 0.0333$ were 0.01, 0.1, 0.15, and 0.2 ml, respectively.

Figure 2 shows a typical example of the process of the crack formation in the final stage of drying the colloidal suspensions via the wetted film. Interestingly, the cracks were introduced along the outer edges first, where dryness proceeds in advance, and the cracks curved and then developed straightforward toward the center of the film. It is also impressive that the new crack developed successively keeping the same angle with the adjacent old crack. The distance between the adjacent cracks, θ should increase as the elastic modulus of the wetted film increases.

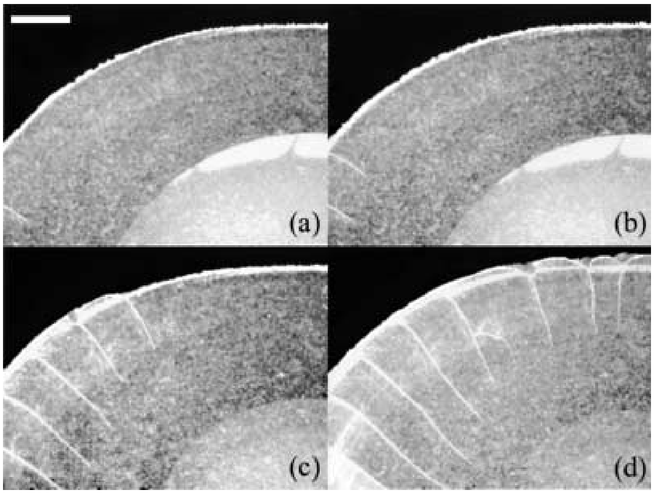

Fig. 2a–d An example of crack formation process for CS-82 spheres on a cover glass at 25 °C: **a** 220 min after dropping suspension; **b** 220 min 40 s; **c** 220 min 50 s; **d** 221 min. In water, $\phi = 0.0333$, 0.3 ml;, length of the *bar* is 1.0 mm

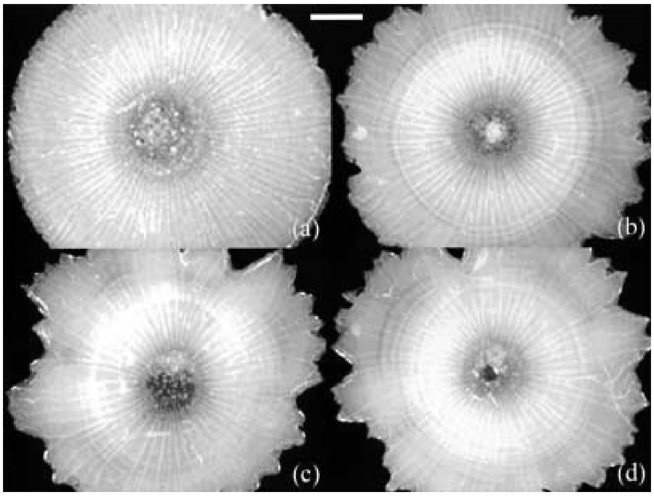

Fig. 3a–d Patterns formed for CS-82 spheres in the presence of sodium chloride on a cover glass at 25 °C. In water, $\phi = 0.0333$, 0.2 ml: **a** [NaCl] = 0 mol/l; **b** 1×10^{-6} mol/l; **c** 1×10^{-5} mol/l; **d** 1×10^{-4} mol/l, length of the *bar* is 2.0 mm

Figure 3 shows the macroscopic patterns formed for the salt-containing suspensions. Clearly, shape of the outer edge changed greatly from the comparatively smooth and round shape to the bumpy one by the addition of sodium chloride. The reason for this observation is not yet clear. However, increase in the air-suspension interface tension by the addition of sodium chloride to the suspension will be one of the main reasons. It should be noted here that the area decreased a bit in the presence of sodium chloride, i.e., the S-values were 95, 91, 88, and 89 mm^2, when the salt concentrations were 0, 10^{-6}, 10^{-5}, and 10^{-4} mol/l, respectively. This decrease is also explainable by the increase of the surface tension in the presence of sodium chloride.

Table 1 shows the influence of the salt concentration on the θ-values. Clearly, the θ-values dropped greatly by the addition of a tiny amount of sodium chloride, 10^{-6} mol/l, and were quite insensitive to the further addition of sodium chloride. This will be due to the decrease in the nearest-neighbored intersphere distance with sodium chloride by the thinning of the electrical double layers around colloidal spheres followed by the increase in the elastic modulus of the film. It is interesting to note that the decrease in the θ-values results from the increase in sphere concentration and/or salt concentration. It should be mentioned further that the d_{max}-values decreased by the addition of sodium chloride. The reason for this observation is not yet clear. However, the accumulation of the spheres by the convection may be retarded by the weakened inter-sphere repulsion.

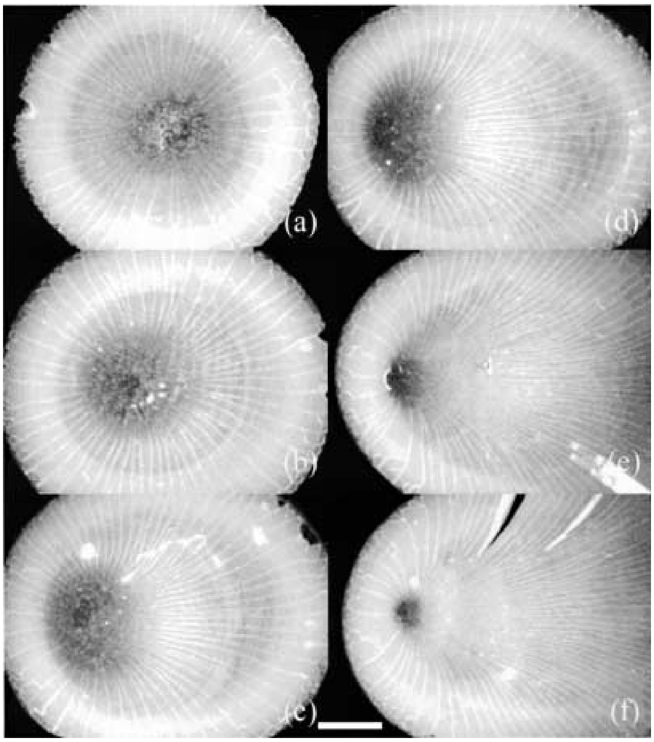

Fig. 5a–f Patterns formed for CS-82 spheres on an inclined cover glass at 25 °C: **a** $\alpha = 0°$; **b** 1.8°; **c** 3.7°; **d** 5.3°; **e** 6.4°; **f** 8°. In water, $\phi = 0.0333$, 0.2 ml, length of the *bar* is 2.0 mm

Table 1 Influence of salt on θ and d_{max}. $\phi = 0.0333$, 0.2 ml

[*NaCl*] (mol/L)	*t* (min)	*S* (mm^2)	θ (degree)	d_{max} (µm)
0	253	95	11.1	135
10^{-6}	263	91	8.34	110
10^{-5}	268	88	8.49	110
10^{-4}	270	89	9.59	115

Next, the influence of inclination of the cover glass upon the macroscopic pattern formation was examined to study the effect of the liquid thickness. Besides the θ-values defined above, the angle of spoke-like cracks from the lowest position, φ and the distance from the center of the film, r were defined as shown in Fig. 4. Figure 5 shows the dissipative structural patterns formed when the inclination angles (α) changed from 0° to 8°. Several characteristic results were obtained. First, location of the pattern center shifted to the lower position as α increased. Second, the θ-values at the low positions increased substantially as α increased, whereas those at the high positions decreased as α increased. Table 2 also clearly shows this tendency of the θ-values. In the low positions, sufficient spheres are supplied in the course of dryness and the shear moduli of the film, which are considered to be the main cause for the crack formation, were high compared with those at the higher positions. Third, the outside pattern shifted from smooth round to

Fig. 4 Setup of cover glass for the inclination experiments and definition of α, φ, θ, and r

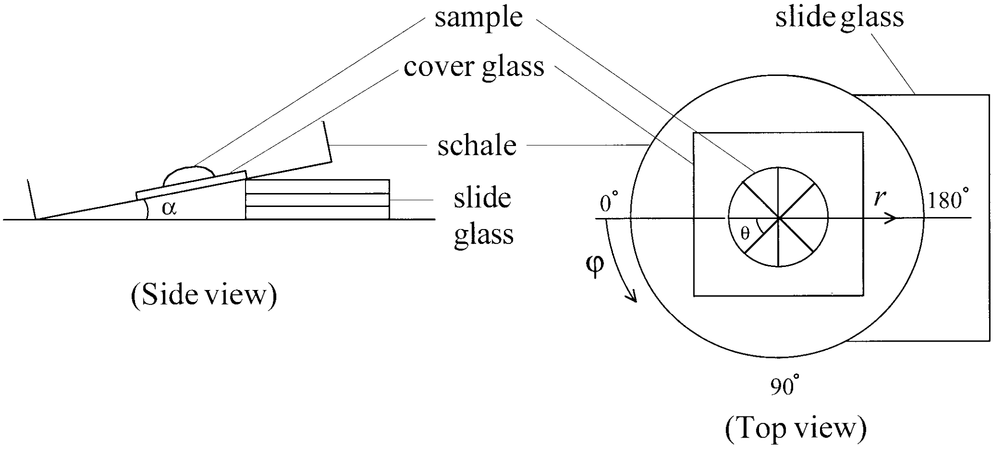

Table 2 Characteristics of the film of CS-82 spheres when the cover glass was inclined in the course of dryness at 25 °C. $\phi = 0.0333$, 0.2 ml

φ (degree)	θ (degree)	d_{max} (µm)
$\alpha = 0°$		
0	10.6	131
45	17.3	168
90	10.1	158
135	11.7	160
180	13.6	137
$\alpha = 1.8°$		
0	13.5	152
45	9.7	144
90	7.9	137
135	5.8	126
180	4.8	115
$\alpha = 8°$		
0	43.7	126
45	10.1	122
90	5.2	91
135	4.0	108
180	2.2	76

the egg-shaped ones, though the shapes of the total pattern are not seen in Fig. 5. Table 2 clearly shows that the d_{max}-values decreased when φ increased in a inclined cover glass. This is also quite understandable since the spheres flow downward.

Area of the patterns increased as α increased, i.e., the S-values were 95, 111, 113, 115, 127, and 137 mm^2 for $\alpha = 0$, 1.8, 3.7, 5.3, 6.4, and 8°, respectively. This inclination effect is quite reasonable when the downward flow of the suspensions is taken into account by the gravity.

The thickness of the film is shown as a function of the distance from the center, r in Fig. 6. The experiments were made directly by taking a close-up CCD picture of the film section, which was stripped off from the cover glass and the section of the cracks appeared often. Plus or minus signs of the r-values in Fig. 6 indicate that the observed position is higher or lower than the center, respectively. Clearly, the thick ring pattern appeared at the outside edge irrespective of α-values. When the cover glass was inclined at $\alpha = 6.4°$, the double peaks in the thickness height were observed at the upper region as is clear in the figure.

Microscopic patterns

Figure 7 shows the patterns formed for the films from the suspensions of comparatively low sphere concentration at $\phi = 1.33 \times 10^{-3}$. Black parts are occupied with the colloidal spheres and the white regions are vacancy parts of spheres on a cover glass. Clearly, the mud cracks are formed. The concentrations ranging from 10^{-6} to 10^{-3} in volume fraction were most appropriate for the formation of the fractal patterns. These microscopic crack patterns seem to be fractal. The fractal dimensions of the patterns at the various concentrations of spheres and sodium chloride were estimated to be between 1.3 and 1.9 by the counting method of the number of squares covering colloidal spheres [33]. These values are larger than the fractal dimension of Koch curve, 1.26.

Reflection spectra in the course of dryness

Figure 8 shows the reflection spectra in the course of dryness at the center of the pattern. Clearly, the peak wavelength (λ_p) shifted first to the longer wavelengths, and then turned to the shorter regions drastically with

Fig. 6 Thickness of the film formed for CS-82 spheres as a function of the distance from the center at 25 °C. In water, $\phi = 0.0333$, 0.2 ml, O: $\alpha = 0°$, X: 6.4°

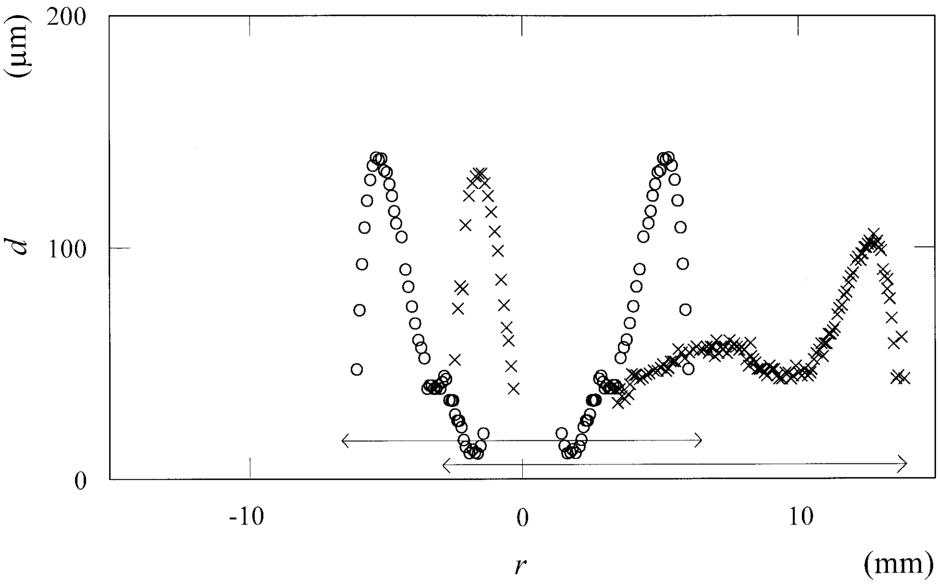

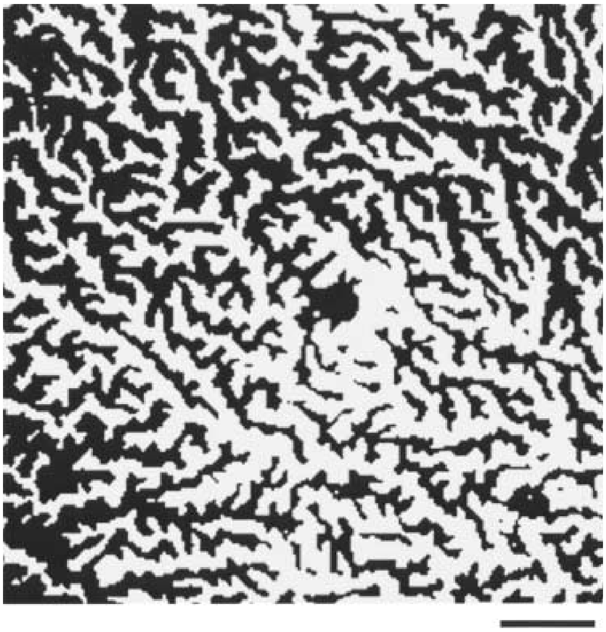

Fig. 7 Patterns formed for CS-82 spheres on a cover glass at 25 °C. In water, $\phi = 1.33\times10^{-3}$, 0.1 ml, length of the *bar* is 20 μm

time, which are also shown in the λ_p-values in Table 3 at $r = 0$. These observations show that the sphere concentration at the center decreases slightly at the initial stage and then increases monotonously. Just before the completion of the dryness at the center the reflection spectra become broad. However, the reflection peaks remained even after the completion of dryness. These observations clearly show that almost all the spheres at the center region go away toward the outside by the convection flow. The reflection spectra in the course of dryness were also taken at $r = 1.5$ and 3.0 mm as is shown in Table 3. In these experiments the spectra kept sharp and shifted toward shorter wavelengths monotonically in the course of dryness. It is interesting to note that the dried up film still shows the reflection peaks indicating the existence of the crystal-like structures in the film. The crystal-like arrangement of the polystyrene spheres dried in a cover glass has been reported [34].

The most reliable inter-sphere distance (l_{obs}) and effective sphere concentration-values (ϕ_{obs}) were obtained by the several repeated calculations from the observed λ_p value and the old n value using Eqs. (1) (2) and compiled in Table 3:

$$l_{obs} = 0.6124\lambda_p/n \tag{1}$$

$$n = \phi \times [\text{refractive index of silica}] + (1 - \phi) \times [\text{refractive index of water or air}] \tag{2}$$

Here, refractive indices of silica, water, and air were assumed to be 1.5, 1.33, and 1.0, respectively. Clearly the l_{obs} values decreased from the initial one corresponding to $\phi = 0.05$ to those of the dried film, i.e., 115, 109, and 106 nm at $r = 0$, 1.5, and 3.0 mm, respectively. These values of the dried film agree excellently with the diameter of the colloidal spheres (103 nm), which shows that the neighbored spheres almost contact each other, keeping crystal-like structure. Observation with an atomic force microscope also supported the contact of the spheres for the dried films. The spheres in the dried film have been reported to distribute in the closed-packed structure from the transmitted-light intensity measurement [34]. The ϕ_{obs}-values of the film were close to but slightly smaller than that of the close-packed fcc lattice, 0.72.

L in Table 3 indicates the size of the single crystals observed from the reflection spectroscopy using the half-width of the reflection peaks or from the CCD pictures

Fig. 8 Reflection spectra of the film formed for CS-82 spheres on a cover glass at 25 °C. In water, $\phi = 0.05$, 0.05 ml, at $r = 0$. Curve (1) $t = 0$ min, (2) 20 min, (3) 40 min, (4) 60 min, (5) 80 min, (6) 100 min, (7) 120 min, (8) 140 min, (9) 160 min

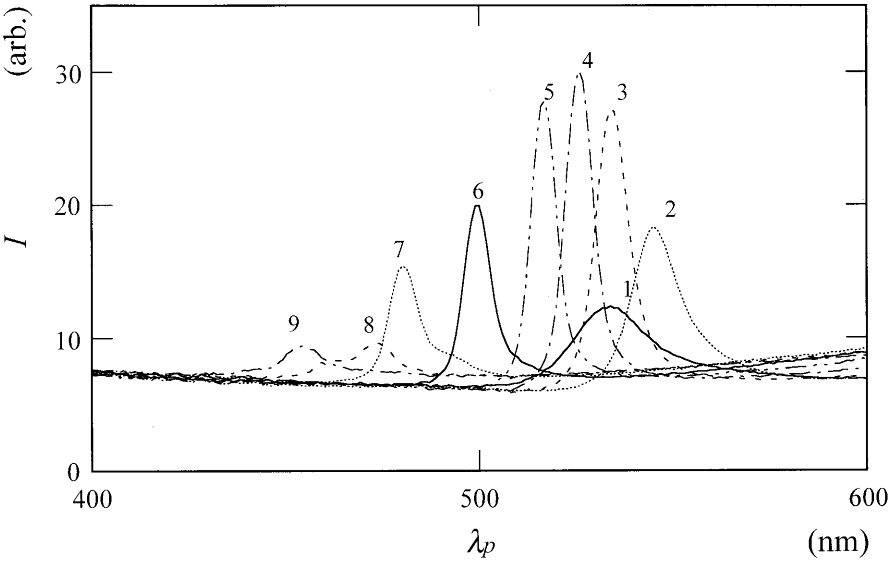

Table 3 Characteristics of the film of CS-82 spheres from reflection spectroscopy. $\phi = 0.05$, 0.05 ml

t (min)	λ_p (nm)			l_{obs} (nm)			ϕ_{obs}			L (μm)			L^a (μm)
	r (mm) = 0	1.5	3.0	0	1.5	3.0	0	1.5	3.0	0	1.5	3.0	0
0	534	534	533	244	244	244	0.056	0.056	0.056	13	10	27	29
20	545	531	509	249	243	232	0.052	0.057	0.064	21	23	41	29
40	534	520	499	244	238	228	0.056	0.060	0.068	29	31	32	32
60	526	503	457	240	230	208	0.058	0.067	0.090	32	31	21	35
80	517	492	423	236	224	192	0.061	0.071	0.11_4	35	27	19	29
120	480	443	402	219	201	182	0.077	0.099	0.13_4	24	15	16	27
160	454	356	391	207	160	177	0.092	0.19_8	0.14_6	–	–	–	–
10080	238	234	232	115	109	106	0.52_9	0.61_6	0.67_7	2.3	3.6	4.8	–

[a] From CCD observation

directly. The latter method gave L-values, being not so sensitive to the time passed. However, two methods gave quite similar values to each other.

Acknowledgments Drs M. Komatsu and M. Hirai of Catalysts & Chemicals Ind. Co. (Tokyo and Kitakyusyu) are sincerely thanked for providing the silica spheres. The Ministry of Education, Science, Sports and Culture is thanked for Grants-in-Aid for Scientific Research on Priority Area (A) (11167241) and for Scientific Research (B) (11450367). T. O. greatly appreciate the late Professor Emeritus Sei Hachisu for his continual encouragement and comments on our work.

References

1. Vanderhoff W, van de Hul HJ, Tausk RJM, Overbeek JTG (1970) Clean surfaces: their preparation and characterization for interfacial studies. Goldfinger G (ed). Dekker, New York
2. Hiltner PA, Papir YS, Krieger IM (1971) J Phys Chem 75:1881
3. Kose A, Ozaki M, Takano K, Kobayashi Y, Hachisu S (1973) J Colloid Interface Sci 44:330
4. Mitaku S, Ohtsuki T, Kishimoto A, Okano K (1980) Biophys Chem 11:411
5. Lindsay HM, Chaikin PM (1982) J Chem Phys 76:3774
6. Pieranski P (1983) Contemp Phys 24:25
7. Ottewill RH (1985) Ber Bunsenges Phys Chem 89:517
8. Aastuen DJW, Clark NA, Cotter LK, Ackerson BJ (1986) Phys Rev Lett 57:1733
9. Pusey PN, van Megen W (1986) Nature (London) 320:340
10. Okubo T (1988) Acc Chem Res 21:281
11. Vanderhoff JW (1973) J Polymer Sci Symp 41:155
12. Nicolis G, Prigogine I (1977) Self-organization in non-equilibrium systems. Wiley, New York
13. Cross MC, Hohenberg (1993) Rev Mod Phys 65:851
14. Ohara PC, Heath JR, Gelbart WM (1997) Angew Chem 109:1120
15. Ohara PC, Heath JR, Gelbart WM (1998) Langmuir 14:3418
16. Uno K, Hayashi K, Hayashi T, Ito K, Kitano H (1998) Colloid Polymer Sci 276:810
17. Gelbart WM, Sear RP, Heath JR, Chang S (1999) Faraday Discuss 112:299
18. van Duffel B, Schoonheydt RA, Grim CPM, De Schryver FC (1999) Langmuir 15:7520
19. Maenosono S, Dushkin CD, Saita S, Yamaguchi Y (1999) Langmuir 15:957
20. Brock SL, Sanabria M, Suib SL, Urban V, Thiyagarajan P, Potter DI (1999) J Phys Chem 103:7416
21. Nikoobakht B, Wang ZL, El-Sayed MA (2000) J Phys Chem 104:8635
22. Ge G, Brus L (2000) J Phys Chem 104:9573
23. Chen KM, Jiang X, Kimerling LC, Hammond PT (2000) Langmuir 16:7825
24. Lin XM, Jaenger HM, Sorensen CM, Klabunde (2001) J Phys Chem 105:3353
25. Kokkoli E, Zukoski CF (2001) 17:369
26. Ung T, Liz-Marzan LM, Mulvaney P (2001) J Phys Chem B 105:3441
27. Shimomura M, Sawadaishi T (2001) Curr Opin Coll Interf Sci 6:11
28. Gunnars J, Stahle P, Wang TC (1997) Comput Mech 19:545
29. Colina H, Roux S (2000) Eur Phys J E 1:189
30. Okubo T, Kimura K, Kimura H (2002) (in preparation)
31. Okubo T, Kimura T, Hayakawa F, Kimura H (2002) (in preparation)
32. Latterini L, Blossey R, Hofkens J, Vanoppen P (1999) Langmuir 15:3582
33. Falconer KJ (1985) The geometry of fractal sets. Cambridge University Press
34. Okubo T (1986) J Chem Soc Faraday Trans 1 82:3175